J Herbmed Pharmacol. 2024; 13(2): 269-279.

http://www.herbmedpharmacol.com doi: 10.34172/jhp.2024.49332

Journal of Herbmed Pharmacology

Deciphering the molecular pathway of an asiaticoside-rich fraction of *Centella asiatica* as an anti-melanogenesis agent

Agustina Setiawati[1], Brigitta Amanda Maharani[1], Putu Addelia Puspa Sari[1], K. Ariex Widyantara[1], Bakti Wahyu Saputra[1], Rifki Febriansyah[2], Rini Dwiastuti[1*]

[1]Faculty of Pharmacy, Sanata Dharma University, Paingan, Maguwoharjo, Depok, Sleman, Yogyakarta, 55282, Indonesia
[2]Faculty of Medicine and Health Sciences, University of Muhammadiyah Yogyakarta, Kasihan, Bantul, Yogyakarta 55183, Indonesia

ARTICLE INFO

Article Type:
Original Article

Article History:
Received: 26 October 2023
Accepted: 25 January 2024

Keywords:
Skin lightening
Anti-hyperpigmentation
Natural product
Skincare
Melanin

ABSTRACT

Introduction: Melanin is a defense against UV radiation; however, it leads to significant cosmetic issues mainly melasma and hyperpigmentation. This study evaluated the potential effect of ethyl acetate (EtOAc) fraction of *Centella asiatica* extract *in vitro* inhibition activity against tyrosinase (TYR). Bioinformatics and *in silico* experiments were also employed to predict molecular pathways of asiaticoside, as the main active compound.
Methods: *Centella asiatica* was extracted with ethanol and then fractionated with EtOAc. The fraction was tested *in vitro* for TYR inhibitory activity, and its active compounds were investigated using thin-layer chromatography (TLC). After obtaining the online database of the genes related to pigmentation and melanogenesis in the skin, the genes affected by asiaticoside were determined by the Venn diagram. The top 10 target proteins, underlying molecular pathways, got from CytoHubba, were further studied to figure out their molecular pathway. The molecular docking was conducted on two selected protein targets.
Results: EtOAc fraction of *C. asiatica* extract demonstrated strong TYR inhibitory activity with an IC_{50} of 18.85 µg/mL. TLC profiling of the EtOAc fraction revealed the *Rf* value of 0.28 for the standard, *Rf* value of 0.26, 0.21, and 0.15 for the extract, and *Rf* value of 0.26 and 0.15 for the fraction. Asiaticoside inhibited melanogenesis by elaborating many molecular pathways involving keratinocytes, melanocytes, fibroblast, and endothelial cells by elaborating cytokine, growth factor, extracellular matrix, and melanin degradation enzyme
Conclusion: Asiaticoside-rich *C. asiatica* fraction has the potential as an anti-melanogenesis agent through its TYR inhibitory activity and many molecular pathways.

Implication for health policy/practice/research/medical education:
Centella asiatica ethyl acetate fraction inhibits melanogenesis by elaborating molecular pathways related to melanin synthesis in vitro and silico. This study confirms that *C. asiatica* is a promising candidate for anti-hyperpigmentation products.
Please cite this paper as: Setiawati A, Maharani BA, Sari PAP, Saputra BW, Febriansah R, Dwiastuti RD. Deciphering the molecular pathway of an asiaticoside-rich fraction of *Centella asiatica* as an anti-melanogenesis agent. J Herbmed Pharmacol. 2024;13(2):269-279. doi: 10.34172/jhp.2024.49332.

Introduction

Melanogenesis is a process of synthesizing melanin by melanocytes, which occurs in the epidermis, the outermost layer of the skin. This epidermal layer is responsible for determining skin color in humans (1,2) involving tyrosinase (TYR), tyrosinase-related protein 1 (TRP1), and tyrosinase-related protein 2 (TRP2) as pivotal enzymes (2,3). The activity of melanin-producing enzymes is distinctly controlled by environmental influences, such as exposure to UV radiation (UVR), as well as internal factors (3). Melanogenesis of pigmentation serves as a defense mechanism for the skin against the damaging effects of UV radiation. Nevertheless, an overproduction of melanin can lead to significant cosmetic issues, such as melasma, freckles, and post-inflammatory hyperpigmentation (4). Therefore, recent studies have been designed to discover novel anti-melanogenesis agents from natural products to reduce hyperpigmentation without inducing toxicity (1).

***Corresponding author**: Rini Dwiastuti,
Email: rini_dwi@usd.ac.id

Numerous compounds that act as biological reducing agents and inhibitors of TYR, like kojic acid (KA), sulfite, and arbutin, have been synthesized to improve conditions of excessive pigmentation and skin discoloration due to disease (5,6). Nevertheless, skin whitening products containing potent TYR inhibitors often come with severe side effects and issues, such as being highly toxic to cells and prone to instability when exposed to oxygen and water, which restricts their practical use (5,6). Numerous natural compounds such as polyphenols, flavonoids, aloesin, and mulberry have been investigated for their potential in addressing skin pigmentation disorders through anti-melanogenesis treatment (7).

One of the promising plants as a natural skin-lightening product is *Centella asiatica,* which has been reported to have a wide range of pharmacological activities, primarily wound healing (8,9), anti-hypertension (10), cardioprotective, neuroprotective, hepatoprotective, antifibrotic, antibacterial, anti-inflammatory, anxiolytic, anti-oxidant, anti-allergic, anti-depressant, anti-arthritic, immunomodulatory, and anti-tumor activities (11). Asiaticoside is the main active compound in *Centella asiatica* along with madecassic acid, madecassoside, and asiatic acid (12). Madecassoside, one of the principal compounds in *C. asiatica*, inhibited melanogenesis and ultraviolet-induced inflammation through the inhibition of protease-activated receptor-2 (PAR-2) expression and its signaling pathways, cyclooxygenase-2 (COX-2), prostaglandin E2, and prostaglandin F2 (13). Asiaticoside was previously *in vivo* studied to inhibit melanogenesis by inhibiting TYR protein and mRNA expression in melanoma (14). In a previous *in silico* study by Hariyono et al, asiaticoside F in *Centella asiatica* exhibited inhibition activity against TYR enzyme (15). However, its *in vitro* activity directly against TYR, and its comprehensive molecular pathways have not been further investigated. This study aimed to comprehensively explore the molecular pathways of the asiaticoside-rich fraction of *C. asiatica* using bioinformatics and *in silico* testing and also assess the TYR inhibitory activity *in vitro*. The result provides more specific data on natural product compounds compared to whole extracts, focusing on a natural ingredient. asiaticoside in *C. asiatica* is suitable for cosmetics, aligning with the growing popularity of safe and effective natural ingredients (16,17). The chemical diversity and bioactive properties of natural products, especially plant extracts, make them preferable in skin care (18-20).

Materials and Methods

Materials

Centella asiatica herb was purchased from the Center for Research and Development of Medicinal Plants and Traditional Medicine (B2P2TOOT), Tawangmangu, Indonesia with authentication number 01/LKTO/Far-USD/VI/2023. A herbarium sample was kept in the same place with the same number. The ethanol (Smart-Lab A-1035) was used for extracting *C. asiatica* herb, while the solvents used for fractionation were hexane (Smart-Lab A-1045) and ethyl acetate (EtOAc) (Smart-Lab A1038) at pro analyst grade and the stationary phase was dry silica gel 60 (70–230 mesh, Supelco 288624). The stationary phase of thin-layer chromatography (TLC) was silica gel GF254 (Sigma-Aldrich) and the mobile phase was hexane, EtOAc, and diethylamine (Merck 8.03010.1000). A TYR inhibition assay kit was purchased from Sigma-Aldrich (MAK257-1KT). The 96-well plate was Corning, all tips were Biologix, and the e-tubes were Axigen.

Extraction and fractionation

The aerial parts of dried *C. asiatica* were collected, ground, and passed through a 60-mesh sieve. The dried powder was macerated by ethanol 70% (1:5 w/v ratio) for 24 hours on a shaker. The residue was remacerated two times using the same solvent. All filtrates were collected using Whatman no. 1 filter paper and evaporated using a rotary evaporator. All of the extract was evaporated using a rotary evaporator followed by drying in the oven at 50 °C until reached a constant weight. The yield of the extraction was reported as the rendering of the extract (8,10,21,22). The extract was fractionated using vacuum liquid chromatographic (VLC). VLC apparatus was prepared by packing a short column with a glass frit (Buchner funnel) using filter papers and 100 g dry silica gel 60 (70–230 mesh) in between. The column was developed by rinsing the silica gel with hexane (100 mL). After the silica gel was free from any solvent, the concentrated crude extract in ethanol was mixed with silica gel until free flow. The free-flow extract was added to the top of the developed column. The mobile phase was added portion by portion in sequence and drawn gently under a vacuum to collect each portion separately. The solvent system used for VLC was hexane, hexane–ethyl acetate (1:1), and EtOAc. The weight of the EtOAc fraction was recorded to determine the yield after evaporation using a Rotavapor to remove the solvents (8,22).

Thin layer chromatography

The EtOAc fraction of *C. asiatica* was subjected to phytochemical screening using TLC to detect the existence of asiaticoside. The asiaticoside test involved TLC with a mobile phase of hexane: EtOAc: diethylamine at a ratio of 80:20:2 (v/v) on silica gel GF254, which was priorly activated at 110 °C for 30 minutes. To perform these tests, 5 µL of both the sample and control solutions were applied to the TLC plate using a micropipette and allowed to develop. The retention factors of the fraction and control were determined and compared to ascertain the presence of asiaticoside by observing under UV 366 nm (22).

In vitro tyrosinase inhibition assay

The *in vitro* TYR inhibition activity of the fraction was

tested based on a colorimetric assay using L-tyrosine as the substrate. Kojic acid was used at a concentration of 0.75 mM. TYR substrate was prepared in the TYR assay buffer with an enhancer at a 2:23:5 v/v ratio. Subsequently, the fraction was added at concentrations of 0.1, 1, 10, 100, and 1000 µg/mL in the TYR buffer, and KA was added in the amount of 20 µL to a 96-well plate. The TYR enzyme solution was then added to each well, and the plate was incubated for 10 minutes at 25°C. Furthermore, 30 µL of L-tyrosinase was pipetted into the well plate. The absorbance of each well was measured using a multi-mode reader (Allsheng FlexA-200) within a range of 30 to 60 minutes. The percentage of relative inhibition was calculated based on the following formula:

$$\%Relative\ Inhibiton = \frac{(Slope\ (EC) - Slope\ (S))}{Slope\ (EC)} \times 100\%$$

Data mining and collection

Before initiating the analysis, the data on proteins and genes involved in pigmentation and melanogenesis were compiled from reputable sources such as PubMed (https://www.ncbi.nlm.nih.gov/), OMIM (https://www.omim.org/), and GeneCard (https://www.genecard.org/). Subsequently, the proteins and genes affected by asiaticoside (AT), both directly and indirectly were screened, using the STITCH database (http://www.stitch.embl.de/). Venn diagram (https://www.interactivenn.net/) was used to determine the overlap of genes affected by KA in the context of pigmentation and melanogenesis (23).

Protein-protein interaction network and gene clustering

The protein-protein interactions (PPI) were unveiled by utilizing the https://www.string-db.org/ platform. This study analyzed the PPI network by https://www.string-db.org/ with a PPI enrichment *P* value of $<10^{-6}$. Following this, the data was processed and analyzed using Cytoscape 3.9.1 and STRING-DB v11.5 software (24,25). To pinpoint the top 15 genes, this study employed the MCC and degree algorithms from the Cyto-Hubba plugin, which were used to categorize them as hub genes (26).

In silico molecular docking

Proteins tumor necrosis factor alpha (TNF-α, PDB ID 2AZ5) and MMP-9 (PDB ID 6ESM) were obtained from www.rcsb.org. The ligands were individually extracted and protonated from these macromolecules using BIOVIA Discovery Studio 2021 for control dockings. The ligands were further processed, including the addition of Gasteiger charges and the incorporation of Kollman charges, which was performed using AutodockTools 1.5.7 (27). The grid box was adjusted, with the center of coordinates set to x = -19.163, y = 74.451, and z = 33.837 for TNF-α, and x = 0.794, y = 50.361, and z = 19.921 for MMP-9. The grid was defined with a size of 50 × 50 × 50 grid points, and the grid point spacing was 0.375 Å. Molecular docking simulations were executed using AutoDock-GPU, involving 1000 iterations (28). The free energy of binding was computed as a sum of various energy components. To evaluate the docking results, the docking poses were visually inspected with BIOVIA Discovery Studio 2021. The RMSD value between the initial and post-docking poses needed to be less than or equal to 2.0 Å (29). For cross-dockings, the ligands were downloaded from PubChem (https://pubchem.ncbi.nlm.nih.gov/), and the same parameters as those used in the control dockings were applied for their preparation and docking.

Results

Centella asiatica extraction and fractionation

Our study initiated the process by exploiting ethanolic extract of *C. asiatica* herbs. Subsequently, we subjected the extract to fractionation using EtOAc to isolate the potentially active compound, asiaticoside. To qualitatively determine the constituents of this fraction, we conducted TLC. The anti-melanogenesis properties of the EtOAc fraction were then confirmed through *in vitro* TYR inhibition assay. Furthermore, to explore the molecular pathway of melanogenesis, the inhibition was investigated using bioinformatics analysis (upper part of Figure 1a). To ensure the preservation of the active compound's integrity during the extraction procedure, we first dried the fresh leaves in an oven, then powdered them, and finally extracted them using ethanol maceration. The resulting extract exhibited a viscous and dark brown appearance and yielded 27.95% w/w extract of dry herbs. The extract was then fractionated using VLC with a stationary phase of silica gel and mobile phases of 100% hexane, hexane-ethyl acetate (50:50), and 100% EtOAc. The EtOAc fraction was 1.196%, resulting in a fraction of 0.0299 g. The EtOAc fraction, which was expected to contain the active leaf compounds, displayed a lighter color in comparison to the initial extract, suggesting that it contained specific compounds with distinct polarity (bottom part of Figure 1a). Figure 1b shows the photograph of an asiaticoside standard, extract, and EtOAc fraction with the *Rf* value of 0.28 for the standard, *Rf* values of 0.26, 0.21, and 0.15 for the extracts, and *Rf* values of 0.26 and 0.15 for the fraction.

In vitro tyrosinase inhibition assay

In vitro, cell-free TYR inhibition activity was conducted by using L-tyrosine as a substrate, which was added after the sample was mixed with the TYR enzyme previously (Figure 2a). The range of EtOAc fraction concentrations used in this study was in the range of 0.1 to 1000 µg/mL, and KA was used as positive control in a concentration of 0.75 mM or 106.58 µg/mL according to the kit. The fraction exhibited TYR inhibition activity at concentration depending on manner with relative inhibition of 89.49 ± 3.40, 60.47 ± 4.09%, 37.96 ± 2.32%, 23.08 ± 3.33%, and 12.75 ± 1.79% at 1000, 100, 10, and 1 ppm concentration,

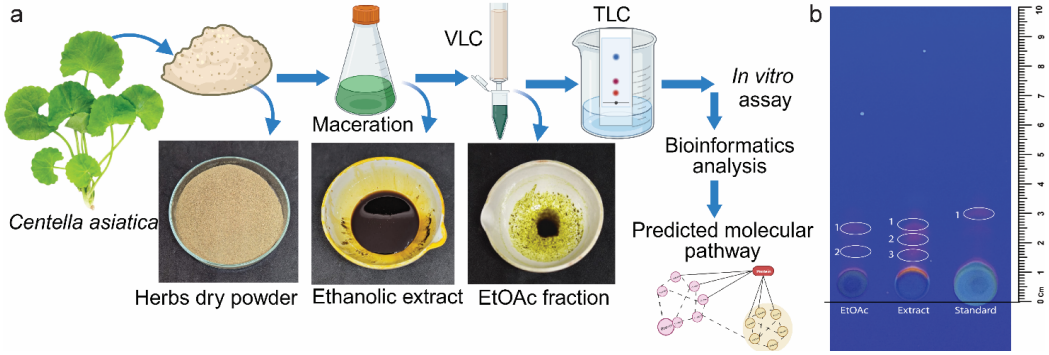

Figure 1. Study scheme of asiaticoside in *Centella asiatica* herb as a natural skin lightening agent. (a) The scheme of this study started from grinding into dry powder, macerating into ethanolic extract, then fractionating with VLC, and its phytochemical compounds were identified with TLC; (b) The TLC of EtOAc fraction. TLC: Thin layer chromatography, VLC: vacuum liquid chromatography; 1: Asiaticoside spot, 2: Madecassoside spot; 3: Asiatic acid spot.

respectively. The higher the concentration of the fraction, the higher the relative inhibition value (Figure 2b). The IC_{50} of the EtOAc fraction was calculated based on the equation of y = 19.087x + 25.66 with a slope of 0.9616, which was previously calculated from the relative inhibition of each fraction concentration (Supplementary file 1). This study revealed that the relative inhibition of EtOAc fraction and asiaticoside at 10 ppm was 37.96 ± 2.32% and 42.79 ± 3.51%, respectively, which was not significantly different. The IC_{50} of EtOAc fraction was 18.85 ppm, while for KA it was 106.58 ppm.

In vitro tyrosinase inhibition assay

In vitro, cell-free TYR inhibition activity was conducted by using L-tyrosine as a substrate, which was added after the sample was mixed with the TYR enzyme previously (Figure 2a). The range of EtOAc fraction concentrations used in this study was in the range of 0.1 to 1000 µg/mL, and KA was used as positive control in a concentration of 0.75 mM or 106.58 µg/mL according to the kit. The fraction exhibited TYR inhibition activity at concentration depending on manner with relative inhibition of 89.49 ± 3.40, 60.47 ± 4.09%, 37.96 ± 2.32%, 23.08 ± 3.33%, and 12.75 ± 1.79% at 1000, 100, 10, and 1 ppm concentration, respectively. The higher the concentration of the fraction, the higher the relative inhibition value (Figure 2b). The IC_{50} of the EtOAc fraction was calculated based on the equation of y= 19.087 + 25.66 with a slope of 0.9616, which was previously calculated from the relative inhibition of each fraction concentration (Supplementary file 1). This study revealed that the relative inhibition of EtOAc fraction and asiaticoside at 10 ppm was 37.96 ± 2.32% and 42.79 ± 3.51%, respectively, which was not significantly different. The IC_{50} of EtOAc fraction was 18.85 ppm, while for KA it was 106.58 ppm. To date, the application of pure asiaticoside or fraction has no difference in TYR inhibition activity. Thus, the fraction exhibited better potential as a TYR inhibitor than KA, a commercial skin-enlightening agent.

Bioinformatics analysis of asiaticoside effect on melanogenesis

Asiaticoside, a triterpene glycoside with the structural formula depicted in Figure 3a, was found through bioinformatic analysis to target 74 genes involved in the

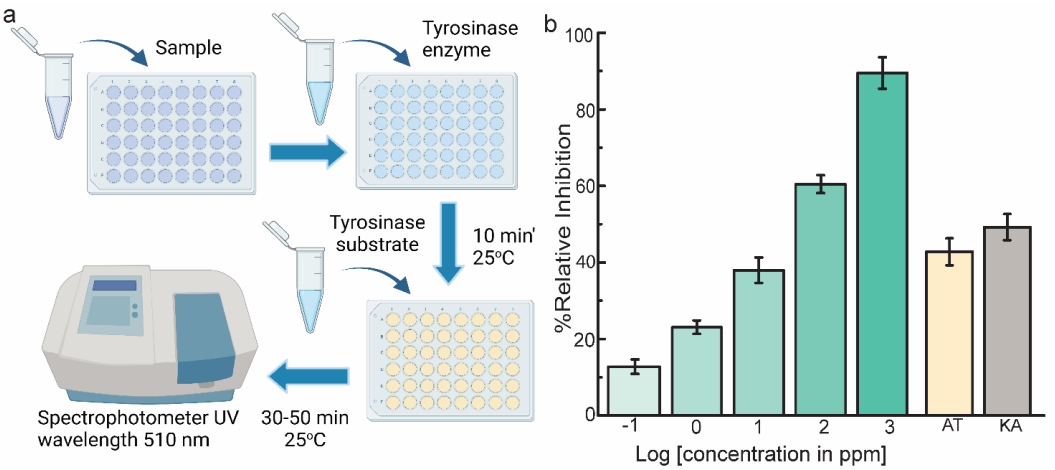

Figure 2. *In vitro* tyrosinase inhibition assay of asiaticoside (AT)-containing fraction. (a) Experiment scheme, (b) Relative inhibition of the fraction at various concentrations. AT was used at 10 ppm and kojic acid (KA) at 0.75 mM as the positive control.

melanogenesis and pigmentation processes out of a total of 12,435 genes (Figure 3b). The number of target genes exceeded that of the positive control, KA. According to the PPI network analysis, these 74 target genes exhibit extensive interactions and form two large interconnected networks. One network is associated with enzyme metabolism (CYP), while the other one is linked to the melanogenesis pathway (Figure 3c). Using Cytoscape and applying the MCC and DMNC algorithms for gene cluster analysis, 15 genes affected by asiaticoside were grouped, resulting in a distinct gene cluster. Based on the MCC algorithm, FN1, VEGFA, MMP9, and TNF achieved the highest scores (Figure 4a). Conversely, according to the DMNC algorithm, MMP1, CXCL1, and CXCL10 were identified as top candidates (Figure 4b).

We further investigated the roles of the top 10 target genes by asiaticoside on the melanogenesis molecular pathway (Table 1). Some of the target genes are cytokines and chemokines such as TNF, IL6, IL1B, CXCL8, and CCL2. All of these cytokines and chemokines are involved upstream in melanogenesis molecular pathways. Moreover, asiaticoside targeted other genes such as FN, MMP9, VEGFA, FGF2, and STAT3.

Furthermore, we selected four proteins, TNF, VEGFR2, MMP-9 (matrix metallopeptidase 9), and STAT3, among the top 15 candidates for analysis using molecular docking with asiaticoside (AT). It displayed binding energy of -9.55, -5.09, -10.43, and -7.35 kcal/mol. AT formed three hydrogen bonds with Gln61, Tyr119, and Tyr151, along with Van der Waals interactions at Leu57, Tyr59, Ser60, Gln61, Ala96, Lys98, Ile118, Leu120, Gly121, Gly122, Val123, and Ile155 residues. Thus, its interaction with VEGFR formed hydrogen bond with Leu840, Cys919, Phe921, Asn923, Thr926, as well as Van der Waals interactions at Lys838, Gly841, Arg842, Val848, Ala866, Val916, Glu917, Phe918, Lys920, Gly922, Tyr927, Arg1032, Leu1035, Ala1050, Arg1051. In contrast, its interaction with MMP-9 resulted in binding energy of -10.43, involving seven hydrogen bonds with Glu186, Tyr218, Val223, Gln227, Tyr245, Pro246, and Tyr248, as well as eleven Van der Waals interactions with Asp185, Leu187, Leu188, Ala189, His190, Leu222, Ala224, His226, Leu243, Met244, and Arg249 residues. Additionally, AT interacted with Ser611, Glu638, Tyr640, Gln644, and Tyr657 through hydrogen bond and with Pro639, Arg609, Glu612, Ser613, Ser614, Thr620, Trp623, Gln235, Ser636, Val637, Thr641, and Ile659 in the STAT3 protein (Table 2).

Discussion

This study screened the EtOAc fraction of *C. asiatica* as a natural anti-melanogenesis agent. The major compound in the fraction is asiaticoside, which also may come along with madecassoside, madecassic acid, and asiatic acid (21). Validation through KLT testing indicates the presence of asiaticoside in both the extract and fraction, with madecassoside exclusively identified in the extract. In both the extract and fraction, an Rf value of 0.26 was assigned to asiaticoside, whereas madecassoside exhibited

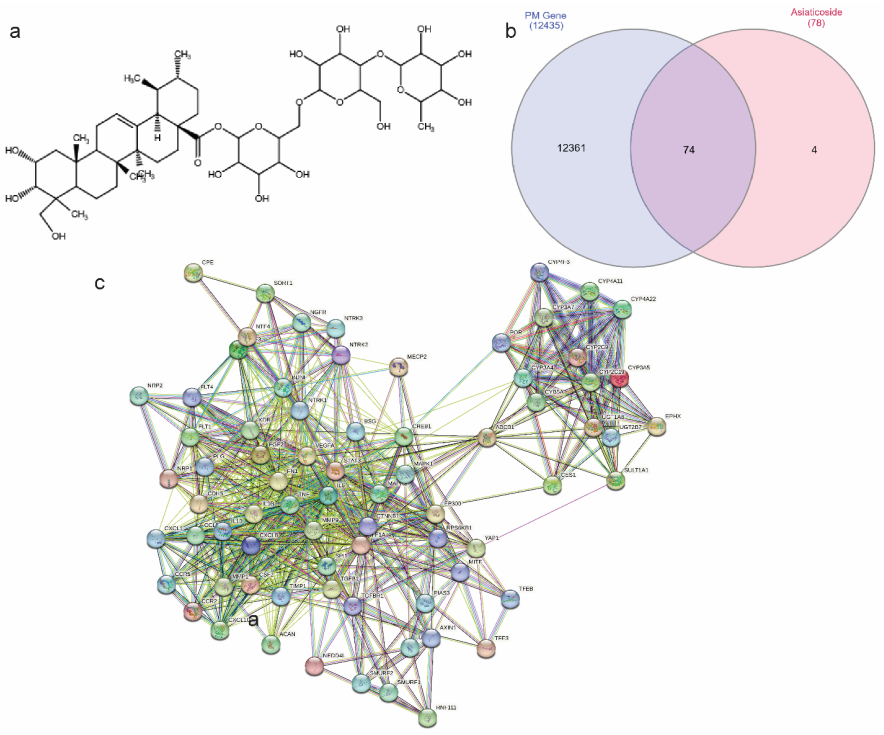

Figure 3. Asiaticoside's top target genes and proteins related to diabetes. (a) Asiaticoside's structure, (b) Venn diagram of asiaticoside and hyperpigmentation interfered genes, (c) Protein-protein interaction (PPI) network of the intersecting genes.

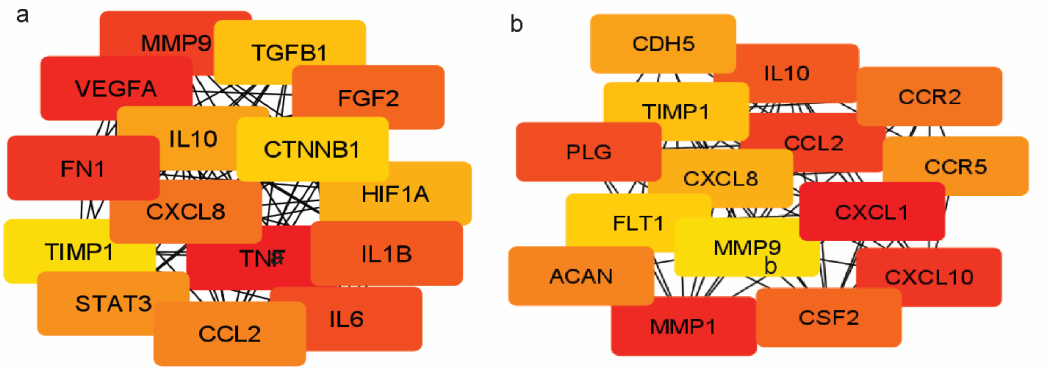

Figure 4. The clustering of the top 15 genes related to melanogenesis and hyperpigmentation according to MCC (a) and DMNC algorithm (b) in CytoHubba. TNF: tumor necrosis factor; VEGFA: vascular endothelial growth factor A; FN1: Fibronectin 1; MMP1/9 : matrix metallopeptidase 1/9; IL6: Interleukin-6; IL1B: Interleukin-1 beta; FGF2: fibroblast growth factor 2; CXCL8/10: C-X-C Motif Chemokine Ligand 8/Interleukin-8; CXCL1: Growth-regulated alpha protein; CCL2: C-C Motif chemokine 2; IL-6/10: Interleukin-6/10; CCR2: C-C chemokine receptor type 2; TIMP1: Metalloproteinase inhibitor 1; CTNNB1: Catenin beta 1; FGF2: Fibroblast growth factor-2; CDH5: Cadherin 5; PLG: Plasmin heavy chain A; CSF2: Granulocyte-macrophage colony-stimulating factor; ACAN: Aggrecan core protein 2; CCR5: C-C chemokine receptor type 5; FLT1: Vascular endothelial growth factor receptor 1.

a closely comparable Rf value to asiaticoside (12). Our study confirmed a previous *in silico* study that asiaticoside F in *C. asiatica* could inhibit TYR enzyme (15). The IC_{50} values obtained from the extractions or fractionations of natural materials are categorized into three groups: IC_{50} values below 100 ppm are classified as strong inhibition, IC_{50} values of 100-450 ppm are classified as moderate inhibition, and IC_{50} values of 450-700 ppm are classified as weak inhibition (45,46). For pure compounds or isolates, the IC_{50} value of 1 µM is considered strong, 1 µM <the IC_{50} 0<10 µM is considered moderate, and IC_{50} > 10 µM is considered weak (47). Asiaticoside-containing EtOAc fraction revealed *in vitro* strong inhibition activity against TYR with an IC_{50} value of 18.85µg/mL, better than KA (IC_{50}= 106.58 µg/mL). The strong inhibition effect of the fraction may be contributed by a compound combination of asiaticoside and madecassoside. A previous study by Cha and colleagues showed that *C. asiatica* extract, containing asiatic acid, asiaticoside, and madecassic acid, impeded melanogenesis in melanoma cell lines (14). Even though madecassoside did not directly target TYR; however, it reduced melanin production and the transfer of melanosomes in a co-culture system of keratinocytes and melanocytes when exposed to UV radiation (13).

Table 1. Top 10 melanogenesis genes affected by asiaticoside based on the maximal clique centrality (MCC) algorithm and their roles in melanogenesis

Gene symbol	Gene/Protein name	Role in melanogenesis	References
TNF	Tumor necrosis factor	Secreted in keratinocytes, inhibit melanogenesis regulation by suppressing the PKA and MAPK pathways.	(30-32)
VEGFA	Vascular endothelial growth factor A	Secreted in keratinocytes, transcripted by STAT3, bind to the receptors, to induce angiogenic cellular responses (proliferation, migration, and sprouting)	(33,34)
FN1	Fibronectin 1	An extracellular matrix (ECM) component, promotes cell rejuvenation, regeneration, proliferation, and migration.	(35-37)
MMP9	Matrix metallopeptidase 9	Secreted in keratinocytes, transcripted by STAT3, degrades the ECM.	(31,38)
IL6	Interleukin-6	Induced by the reaction of NF-kB with TNF and IL1, inhibits melanogenesis regulation by decreasing TYR activity, increasing the production of STAT3	(30,32,39)
IL1B	Interleukin-1 beta	Inhibit melanogenesis regulation by suppressing the MAPK pathway	(30,32,39)
FGF2	Fibroblast growth factor 2	Bind to its receptors, to induce cell repair and remodeling of the skin dermis	(40)
CXCL8	C-X-C Motif chemokine ligand 8/ interleukin-8	Bind to chemokine receptors, increase production of MAPK	(41)
CCL2	C-C Motif chemokine 2	Bind to chemokine receptors, increase production of JAK, which triggers the production of STAT pathway	(42)
STAT3	Signal Transducer and activator of transcription 3	Phosphorylates by JAK2, trigger the production of MITF, as a transcription factor of TYR, TRP-1, and TRP-2, as well as VEGFA	(43,44)

Table 2. Molecular docking results of asiaticoside against tyrosinase

Target protein	Binding energy (kcal/mol)	H-bond residues	Hydrophobic residues	Van der Waals residues
TNF-alpha	-9.55	Gln61, Tyr119, Tyr151	Tyr59, Tyr119, Tyr151	Leu57, Tyr59, Ser60, Gln61, Ala96, Lys98, Ile118, Leu120, Gly121, Gly122, Val123, Ile155
VEGFR2	-5.09	Leu840, Cys919, Phe921, Asn923, Thr926	Leu840, Phe1047	Lys838, Gly841, Arg842,Val848, Ala866, Val916, Glu917, Phe918, Lys920, Gly922, Tyr927, Arg1032, Leu1035, Ala1050, Arg1051
MMP-9	-10.43	Glu186, Tyr218, Val223, Gln227, Tyr245, Pro246, Tyr248	His230, His236, Met247	Asp185, Leu187, Leu188, Ala189, His190, Leu222, Ala224, His226, Leu243, Met244, Arg249
STAT3	-7.35	Ser611, Glu638, Tyr640, Gln644, Tyr657	Pro639	Arg609, Glu612, Ser613, Ser614, Thr620, Trp623, Gln235, Ser636, Val637, Thr641, Ile659

Gln: glutamine; Leu: leucine; Ser: serine; Tyr: tyrosine; Ala: alanine; Ile: isoleucine; Lys: lysine; Glu: glutamine; Val: valine; Pro: proline; His: histidine; Met: methionine; Arg: arginin; Phe: phenylalanin.

Therefore, our study investigated other molecular mechanisms and pathways of compounds in the EtOAc fraction of *C. asiatica* through bioinformatics analysis.

Since the most dominant compound in *C. asiatica* is asiaticoside (14), this study further investigated protein targets to the gene using bioinformatics analysis. In the protein-protein interaction network, this study employed parameters of MCC and DMNC. The MCC data offers a superior analysis compared to other algorithms, as it captures more essential proteins in both high and low-ranking protein lists (26,48). Therefore, the MCC data (maximal clique centrality) serves as a foundation for predicting the top 10 genes and the molecular inhibition pathways of melanogenesis by asiaticoside, drawing on existing literature. The genes affected by asiaticoside were melanogenesis-related genes such as cytokine/chemokine, ECM, and melanin degradation enzyme as well as a transcription factor. Some of the target genes are cytokines and chemokines, which play crucial roles in the upstream molecular pathways associated with melanogenesis (32,49,50). Asiaticoside, on the other hand, specifically targets fibronectin (FN), an extracellular matrix component in skin tissue, along with its degrading enzyme MMP9. FN1 promotes the rejuvenation, regeneration, proliferation, and migration of cells while degrading the extracellular matrix (30,33,35). Consequently, asiaticoside influences growth factors like VEGFA and FGF2, contributing to angiogenesis in endothelial cells and the remodeling of the skin's dermis (23,29). Moreover, asiaticoside shot at STAT3, a transcription factor of some genes related to melanogenesis such as TYR (51,52).

The main target of asiaticoside is TNF-α, an inflammatory cytokine secreted by keratinocytes. Asiaticoside binds to TNF-α in molecular docking analysis. Some references demonstrated the opposite effects of TNF-α, which inhibited the melanogenesis pathway through the inhibition of PKA and MAPK pathways (46,49). However, UV irradiation triggers a subsequent series of TNF-α released by keratinocytes and other cell types, leading to melanogenesis (49). In melanocytes, cytokines bind to their receptor to activate NF-κB, which can induce IL-6 transcription and subsequently activate the transcription factor of STAT3, which can activate MITF (46,49). Subsequently, MITF translocates to the nucleus and serves its function as a transcription factor for TYR, TRP-1, and TRP-2 (36,49,53). Interestingly, STAT3 is directly inhibited by asiaticoside (30). Thus, asiaticoside is predicted to inhibit IL-1β, which subsequently stops α-melanocyte stimulating hormone (MSH) activation to its receptor (54). This pathway activates protein-kinase A (PKA) and MAPK pathway, which activates MITF (55).

Asiaticoside binds to MMP-9, a family of Zn-dependent proteases that is constitutively secreted primarily in leukocytes, whereas most other cell types include keratinocytes (35). It hydrolyses extracellular matrix component, which is mostly produced by fibroblasts in skin tissue (31). In the same cells, asiaticoside induces fibronectin (FN1), a dimmer protein component of ECM, which may undergo polymerization to stimulate cell proliferation and migration (53). Additionally, asiaticoside stimulates FGF-2 to promote cell migration and proliferation, as well as to control cell growth (56) (Figure 5). Therefore, asiaticoside is a potential natural compound for skin rejuvenation. This has been previously demonstrated in our studies (11,57). Thus, FGF-2 also serves as a melanogenesis stimulator in melanocytes. A lower dose of UV radiation-induced FGF-2, which then activates STAT-3 to increase PAX-3, has been shown to regulate melanocyte survival and melanin synthesis (58). To suppress melanogenesis, asiaticoside binding may serve as an inhibitory function against FGF-2 in melanogenesis. Yet, this hypothesis should be answered in upcoming studies.

Through molecular docking analysis, it is found that asiaticoside exhibits inhibitory potential against TNF-α (Figure 6a), VEGFR2 (Figure 6b), MMP-9 (Figure 6c), and STAT3 (Figure 6d). The ribbon diagram illustrates the molecular interaction of asiaticoside within the active site pocket of TNF-alpha, VEGFR2, MMP-9, and STAT3. Both docking configurations against TNF-α, VEGFR2, MMP-

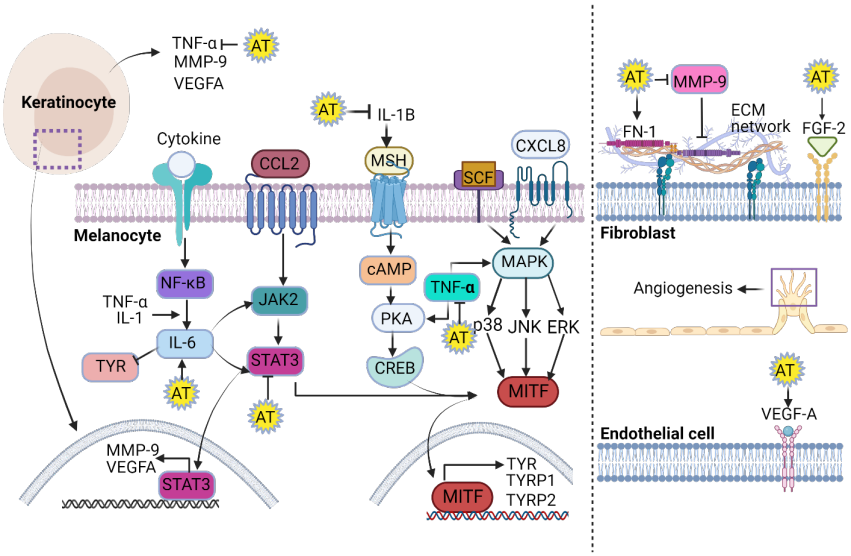

Figure 5. A predicted molecular cascade of asiaticoside (AT) in melanogenesis and pigmentation of the skin. TNF: Tumor necrosis factor; VEGFA: Vascular endothelial growth factor A; FN1: Fibronectin 1; MMP9: Matrix metallopeptidase 9; IL6: Interleukin-6; IL1B: Interleukin-1 beta; FGF2: Fibroblast growth factor 2; CXCL8: C-X-C Motif chemokine ligand 8/interleukin-8; CCL2: C-C Motif chemokine 2; STAT3: Signal transducer and activator of transcription 3; α- MSH: α-Melanocyte-STIMULATING Hormone; SCF: Stem cell factor; NF-kB: nuclear factor-kappaB; TYR: Tyrosinase; TYRP1: Tyrosinase related protein 1; TYRP2: tyrosinase related protein 2; MITF: Master regulator-microphthalmia-associated transcription factor; JAK2: Janus kinase 2; cAMP: Cyclic adenosine monophosphate; PKA: Protein kinase A; CREB: cAMP response element-binding protein; MAPK: Mitogen-activated protein kinases; JNK: c-Jun N-terminal kinase; ERK: Extracellular signal-regulated kinases; ECM: Extracellular matrix. This figure was prepared using BioRender free version (Creative Commons Attribution-NonCommercial license (CC BY-NC).

9, and STAT3 had root mean square deviation (RMSD) values of 1.33, 1.90, 1.91, and 1.89 Å, which is considered valid due to the value under 2.00 Å (59). Asiaticoside may inhibit TNF-α, VEGFR2, MMP-9, and STAT3 by the proteins' active site binding and potential to be further investigated as a clinic skin enlightening agent.

Asiaticoside other that melanocytes, keratinocytes, and fibroblasts, affects endothelial cells. VEGF-A is recognized for its role in facilitating skin regeneration by stimulating the formation of new blood vessels (angiogenesis) on endothelial cells and through direct effects on melanocytes and keratinocytes (52). Asiaticoside is predicted to stimulate VEGF-A production, which may contribute to its activity as skin rejuvenation. Our study revealed that the EtOAc fraction of *C. asiatica* could inhibit melanogenesis by elaborating many molecular pathways involving keratinocytes, melanocytes, fibroblasts, and endothelial cells. Further studies relating to pure compound isolation in *C. asiatica* and their activities against melanogenesis molecular pathways are needed.

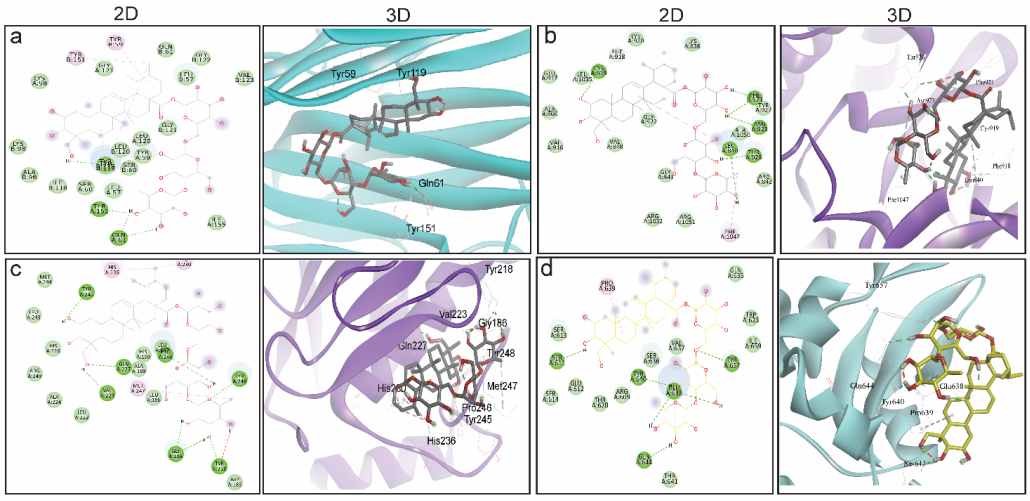

Figure 6. The binding poses of asiaticoside at selected protein in 2D view (left) and 3D view (right) at TNF-α (a), VEGFR2 (b), MMP-9 (c), and STAT3 (d) binding pocket. Yellow, red, and white indicate carbon, oxygen, and hydrogen atoms, respectively. Green, pink, orange, and purple represent Van der Walls, alkyl/pi-alkyl, pi-sulfur, and pi-sigma, respectively.

Conclusion

In vitro tests showed that the EtOAc fraction obtained from *C. asiatica* displayed significant inhibitory activity on TYR, ultimately leading to the suppression of melanogenesis. The *in vitro* study was revealed to contain asiaticoside and madecassoside. Bioinformatics analysis revealed that asiaticoside in *Centella asiatica* exhibited multiple molecular pathways in several skin cells. This study provides a scientific basis for natural product-based skincare, especially focusing on skin-lightening agents.

Authors' contributions

Conceptualization: Rini Dwiastuti, Agustina Setiawati, Rifki Febriansyah.
Data curation: Brigitta Amanda Maharani, K. Ariex Widyantara, Bakti Wahyu Saputra.
Formal analysis : Brigitta Amanda Maharani, K. Ariex Widyantara, Bakti Wahyu Saputra.
Funding acquisition: Rini Dwiastuti, Agustina Setiawati, Rifki Febriansyah.
Investigation: Rini Dwiastuti, Agustina Setiawati.
Methodology: Agustina Setiawati.
Project administration: Putu Addelia Puspa Sari, K. Ariex Widyantara, Rifki Febriansyah.
Resources: Rini Dwiastuti.
Software: K. Ariex Widyantara, Bakti Wahyu Saputra.
Supervision: Agustina Setiawati.
Validation: Agustina Setiawati.
Visualization: Bakti Wahyu Saputra, Agustina Setiawati.
Writing–original draft: Brigitta Amanda Maharani, Bakti Wahyu Saputra.
Putu Addelia Puspa Sari, Agustina Setiawati.
Writing–review & editing: Putu Addelia Puspa Sari, Agustina Setiawati.

Conflict of interests

The authors declare no conflict of interest.

Ethical considerations

This study was performed following the protocols approved by the Ethics Committee of the Faculty of Medicine, Universitas Gadjah Mada of Yogyakarta, Indonesia (Approval No. KE/FK/1135/EC/2022).

Funding/Support

This work was funded by The Directorate of Research, Technology, and Community Services, the Directorate General of Higher Education, Research, and Technology, and the Indonesian Ministry of Education, Culture, Research and Technology with project number 0423.10/LL5-INT/AL.04/2023 and No. 041a Penel./LPPM-USD/VI/2023.

References

1. Qian W, Liu W, Zhu D, Cao Y, Tang A, Gong G, et al. Natural skin-whitening compounds for the treatment of melanogenesis (Review). Exp Ther Med. 2020;20(1):173-85. doi: 10.3892/etm.2020.8687.
2. D'Mello SA, Finlay GJ, Baguley BC, Askarian-Amiri M. Signaling pathways in melanogenesis. Int J Mol Sci. 2016;17(7):1144. doi: 10.3390/ijms17071144.
3. Alam MB, Ahmed A, Motin MA, Kim S, Lee SH. Attenuation of melanogenesis by *Nymphaea nouchali* (Burm. f) flower extract through the regulation of cAMP/CREB/MAPKs/MITF and proteasomal degradation of tyrosinase. Sci Rep. 2018;8(1):13928. doi: 10.1038/s41598-018-32303-7.
4. Gillbro JM, Olsson MJ. The melanogenesis and mechanisms of skin-lightening agents--existing and new approaches. Int J Cosmet Sci. 2011;33(3):210-21. doi: 10.1111/j.1468-2494.2010.00616.x.
5. García-Gavín J, González-Vilas D, Fernández-Redondo V, Toribio J. Pigmented contact dermatitis due to kojic acid. A paradoxical side effect of a skin lightener. Contact Dermatitis. 2010;62(1):63-4. doi: 10.1111/j.1600-0536.2009.01673.x.
6. Pollock S, Taylor S, Oyerinde O, Nurmohamed S, Dlova N, Sarkar R, et al. The dark side of skin lightening: an international collaboration and review of a public health issue affecting dermatology. Int J Womens Dermatol. 2021;7(2):158-64. doi: 10.1016/j.ijwd.2020.09.006.
7. Zhu W, Gao J. The use of botanical extracts as topical skin-lightening agents for the improvement of skin pigmentation disorders. J Investig Dermatol Symp Proc. 2008;13(1):20-4. doi: 10.1038/jidsymp.2008.8.
8. Sh Ahmed A, Taher M, Mandal UK, Jaffri JM, Susanti D, Mahmood S, et al. Pharmacological properties of *Centella asiatica* hydrogel in accelerating wound healing in rabbits. BMC Complement Altern Med. 2019;19(1):213. doi: 10.1186/s12906-019-2625-2.
9. Bylka W, Znajdek-Awiżeń P, Studzińska-Sroka E, Brzezińska M. *Centella asiatica* in cosmetology. Postepy Dermatol Alergol. 2013;30(1):46-9. doi: 10.5114/pdia.2013.33378.
10. Harwoko H, Pramono S, Nugroho AE. Triterpenoid-rich fraction of *Centella asiatica* leaves and in vivo antihypertensive activity. Int Food Res J. 2014;21(1):149-54.
11. Bandopadhyay S, Mandal S, Ghorai M, Jha NK, Kumar M, Radha, et al. Therapeutic properties and pharmacological activities of asiaticoside and madecassoside: a review. J Cell Mol Med. 2023;27(5):593-608. doi: 10.1111/jcmm.17635.
12. Bonfill M, Mangas S, Cusidó RM, Osuna L, Piñol MT, Palazón J. Identification of triterpenoid compounds of *Centella asiatica* by thin-layer chromatography and mass spectrometry. Biomed Chromatogr. 2006;20(2):151-3. doi: 10.1002/bmc.564.
13. Jung E, Lee JA, Shin S, Roh KB, Kim JH, Park D. Madecassoside inhibits melanin synthesis by blocking ultraviolet-induced inflammation. Molecules. 2013;18(12):15724-36. doi: 10.3390/molecules181215724.
14. Kwon KJ, Bae S, Kim K, An IS, Ahn KJ, An S, et al. Asiaticoside, a component of *Centella asiatica*, inhibits melanogenesis in B16F10 mouse melanoma. Mol Med Rep. 2014;10(1):503-7. doi: 10.3892/mmr.2014.2159.
15. Hariyono P, Karamoy JR, Hariono M. Exploration of Indonesian plants as skin lightening against tyrosinase: a virtual screening. Indones J Pharm Sci Technol. 2019;1(2):25-32. doi: 10.24198/ijpst.v1i2.20194.

16. Idris FN, Mohd Nadzir M. Comparative studies on different extraction methods of *Centella asiatica* and extracts bioactive compounds effects on antimicrobial activities. Antibiotics (Basel). 2021;10(4):457. doi: 10.3390/antibiotics10040457.
17. Liu JK. Natural products in cosmetics. Nat Prod Bioprospect. 2022;12(1):40.doi:10.1007/s13659-022-00363-y.
18. Ponphaiboon J, Krongrawa W, Aung WW, Chinatangkul N, Limmatvapirat S, Limmatvapirat C. Advances in natural product extraction techniques, electrospun fiber fabrication, and the integration of experimental design: a comprehensive review. Molecules. 2023;28(13):5163. doi: 10.3390/molecules28135163.
19. Rasoanaivo P, Wright CW, Willcox ML, Gilbert B. Whole plant extracts versus single compounds for the treatment of malaria: synergy and positive interactions. Malar J. 2011;10(Suppl 1):S4. doi: 10.1186/1475-2875-10-s1-s4.
20. Zhang QW, Lin LG, Ye WC. Techniques for extraction and isolation of natural products: a comprehensive review. Chin Med. 2018;13:20. doi: 10.1186/s13020-018-0177-x.
21. Azis HA, Taher M, Ahmed AS, Sulaiman WM, Susanti D, Chowdhury SR, et al. In vitro and in vivo wound healing studies of methanolic fraction of *Centella asiatica* extract. S Afr J Bot. 2017;108:163-74. doi: 10.1016/j.sajb.2016.10.022.
22. Monton C, Settharaksa S, Luprasong C, Songsak T. An optimization approach of dynamic maceration of *Centella asiatica* to obtain the highest content of four centelloids by response surface methodology. Rev Bras Farmacogn. 2019;29(2):254-61. doi: 10.1016/j.bjp.2019.01.001.
23. Vassilev D, Leunissen J, Atanassov A, Nenov A, Dimov G. Application of bioinformatics in plant breeding. Biotechnol Biotechnol Equip. 2005;19(Suppl 3):139-52. doi: 10.1080/13102818.2005.10817293.
24. Shannon P, Markiel A, Ozier O, Baliga NS, Wang JT, Ramage D, et al. Cytoscape: a software environment for integrated models of biomolecular interaction networks. Genome Res. 2003;13(11):2498-504. doi: 10.1101/gr.1239303.
25. Szklarczyk D, Gable AL, Nastou KC, Lyon D, Kirsch R, Pyysalo S, et al. The STRING database in 2021: customizable protein-protein networks, and functional characterization of user-uploaded gene/measurement sets. Nucleic Acids Res. 2021;49(D1):D605-12. doi: 10.1093/nar/gkaa1074.
26. Chin CH, Chen SH, Wu HH, Ho CW, Ko MT, Lin CY. cytoHubba: identifying hub objects and sub-networks from complex interactome. BMC Syst Biol. 2014;8(Suppl 4):S11. doi: 10.1186/1752-0509-8-s4-s11.
27. Morris GM, Huey R, Lindstrom W, Sanner MF, Belew RK, Goodsell DS, et al. AutoDock4 and AutoDockTools4: automated docking with selective receptor flexibility. J Comput Chem. 2009;30(16):2785-91. doi: 10.1002/jcc.21256.
28. Santos-Martins D, Solis-Vasquez L, Tillack AF, Sanner MF, Koch A, Forli S. Accelerating AutoDock4 with GPUs and gradient-based local search. J Chem Theory Comput. 2021;17(2):1060-73. doi: 10.1021/acs.jctc.0c01006.
29. Hevener KE, Zhao W, Ball DM, Babaoglu K, Qi J, White SW, et al. Validation of molecular docking programs for virtual screening against dihydropteroate synthase. J Chem Inf Model. 2009;49(2):444-60. doi: 10.1021/ci800293n.
30. Hossain MR, Ansary TM, Komine M, Ohtsuki M. Diversified stimuli-induced inflammatory pathways cause skin pigmentation. Int J Mol Sci. 2021;22(8):3970. doi: 10.3390/ijms22083970.
31. Boukhedouni N, Martins C, Darrigade AS, Drullion C, Rambert J, Barrault C, et al. Type-1 cytokines regulate MMP-9 production and E-cadherin disruption to promote melanocyte loss in vitiligo. JCI Insight. 2020;5(11):e133772. doi: 10.1172/jci.insight.133772.
32. Fu C, Chen J, Lu J, Yi L, Tong X, Kang L, et al. Roles of inflammation factors in melanogenesis (Review). Mol Med Rep. 2020;21(3):1421-30. doi: 10.3892/mmr.2020.10950.
33. Kontos CD. More than skin deep: connecting melanocyte pigmentation and angiogenic diseases. J Clin Invest. 2014;124(1):76-9. doi: 10.1172/jci73559.
34. Keren A, Bertolini M, Keren Y, Ullmann Y, Paus R, Gilhar A. Human organ rejuvenation by VEGF-A: lessons from the skin. Sci Adv. 2022;8(25):eabm6756. doi: 10.1126/sciadv.abm6756.
35. Gimeno LI, Benito-Jardón M, Guerrero-Barberà G, Burday N, Costell M. The role of the fibronectin synergy site for skin wound healing. Cells. 2022;11(13):2100. doi: 10.3390/cells11132100.
36. Napoli S, Scuderi C, Gattuso G, Bella VD, Candido S, Basile MS, et al. Functional roles of matrix metalloproteinases and their inhibitors in melanoma. Cells. 2020;9(5):1151. doi: 10.3390/cells9051151.
37. Parisi L, Toffoli A, Ghezzi B, Mozzoni B, Lumetti S, Macaluso GM. A glance on the role of fibronectin in controlling cell response at biomaterial interface. Jpn Dent Sci Rev. 2020;56(1):50-5. doi: 10.1016/j.jdsr.2019.11.002.
38. Napolitano A, Ito S. Skin pigmentation: is the control of melanogenesis a target within reach? Int J Mol Sci. 2018;19(12):4040. doi: 10.3390/ijms19124040.
39. Cabaço LC, Tomás A, Pojo M, Barral DC. The dark side of melanin secretion in cutaneous melanoma aggressiveness. Front Oncol. 2022;12:887366. doi: 10.3389/fonc.2022.887366.
40. Upadhyay PR, Ho T, Abdel-Malek ZA. Participation of keratinocyte- and fibroblast-derived factors in melanocyte homeostasis, the response to UV, and pigmentary disorders. Pigment Cell Melanoma Res. 2021;34(4):762-76. doi: 10.1111/pcmr.12985.
41. Campbell LM, Maxwell PJ, Waugh DJ. Rationale and means to target pro-inflammatory interleukin-8 (CXCL8) signaling in cancer. Pharmaceuticals (Basel). 2013;6(8):929-59. doi: 10.3390/ph6080929.
42. Fei L, Ren X, Yu H, Zhan Y. Targeting the CCL2/CCR2 axis in cancer immunotherapy: one stone, three birds? Front Immunol. 2021;12:771210. doi: 10.3389/fimmu.2021.771210.
43. Yoon JH, Youn K, Jun M. Discovery of pinostrobin as a melanogenic agent in cAMP/PKA and p38 MAPK signaling pathway. Nutrients. 2022;14(18):3713. doi: 10.3390/nu14183713.
44. Tanwar J, Sharma A, Saurav S, Shyamveer, Jatana N, Motiani RK. MITF is a novel transcriptional regulator of the calcium sensor STIM1: significance in physiological melanogenesis. J Biol Chem. 2022;298(12):102681. doi: 10.1016/j.jbc.2022.102681.
45. Tahir KA, Miskad UA, Djawad K, Sartini S, Djide NM, Indrisari M, et al. Tyrosinase enzymes activities and sun protection factor of ethanol extract, water fraction, and

n-butanol fraction of *Chromolaena odorata* L. leaves. Open Access Maced J Med Sci. 2021;9(A):493-8. doi: 10.3889/oamjms.2021.6226.
46. Batubara I, Darusman LK, Mitsunaga T, Rahminiwati M, Djauhari E. Potency of Indonesian medicinal plants as tyrosinase inhibitor and antioxidant agent. J Biol Sci. 2010;10(2):138-44. doi: 10.3923/jbs.2010.138.144.
47. Krippendorff BF, Lienau P, Reichel A, Huisinga W. Optimizing classification of drug-drug interaction potential for CYP450 isoenzyme inhibition assays in early drug discovery. J Biomol Screen. 2007;12(1):92-9. doi: 10.1177/1087057106295897.
48. Lin CY, Chin CH, Wu HH, Chen SH, Ho CW, Ko MT. Hubba: hub objects analyzer--a framework of interactome hubs identification for network biology. Nucleic Acids Res. 2008;36(Suppl 2):W438-43. doi: 10.1093/nar/gkn257.
49. Yang CY, Guo Y, Wu WJ, Man MQ, Tu Y, He L. UVB-induced secretion of IL-1β promotes melanogenesis by upregulating TYR/TRP-1 expression in vitro. Biomed Res Int. 2022;2022:8230646. doi: 10.1155/2022/8230646.
50. Choi H, Choi H, Han J, Jin SH, Park JY, Shin DW, et al. IL-4 inhibits the melanogenesis of normal human melanocytes through the JAK2-STAT6 signaling pathway. J Invest Dermatol. 2013;133(2):528-36. doi: 10.1038/jid.2012.331.
51. Yang CH, Fan M, Slominski AT, Yue J, Pfeffer LM. The role of constitutively activated STAT3 in B16 melanoma cells. Int J Interferon Cytokine Mediat Res. 2010;2010(2):1-7. doi: 10.2147/ijicmr.s6657.
52. Niu C, Aisa HA. Upregulation of melanogenesis and tyrosinase activity: potential agents for vitiligo. Molecules. 2017;22(8):1303. doi: 10.3390/molecules22081303.
53. Costin GE, Hearing VJ. Human skin pigmentation: melanocytes modulate skin color in response to stress. FASEB J. 2007;21(4):976-94. doi: 10.1096/fj.06-6649rev.
54. Slominski A, Tobin DJ, Shibahara S, Wortsman J. Melanin pigmentation in mammalian skin and its hormonal regulation. Physiol Rev. 2004;84(4):1155-228. doi: 10.1152/physrev.00044.2003.
55. Lajis AF, Hamid M, Ariff AB. Depigmenting effect of Kojic acid esters in hyperpigmented B16F1 melanoma cells. J Biomed Biotechnol. 2012;2012:952452. doi: 10.1155/2012/952452.
56. Bikfalvi A, Klein S, Pintucci G, Rifkin DB. Biological roles of fibroblast growth factor-2. Endocr Rev. 1997;18(1):26-45. doi: 10.1210/edrv.18.1.0292.
57. Park KS. Pharmacological effects of *Centella asiatica* on skin diseases: evidence and possible mechanisms. Evid Based Complement Alternat Med. 2021;2021:5462633. doi: 10.1155/2021/5462633.
58. Dong L, Li Y, Cao J, Liu F, Pier E, Chen J, et al. FGF2 regulates melanocytes viability through the STAT3-transactivated PAX3 transcription. Cell Death Differ. 2012;19(4):616-22. doi: 10.1038/cdd.2011.132.
59. Zhong H, Wang Z, Wang X, Liu H, Li D, Liu H, et al. Importance of a crystalline water network in docking-based virtual screening: a case study of BRD4. Phys Chem Chem Phys. 2019;21(45):25276-89. doi: 10.1039/c9cp04290c.